Catalytic consequences of open and closed grafted Al(III)-calix[4]arene complexes for hydride and oxo transfer reactions

Partha Nandi[a,1], Wenjie Tang[b], Alexander Okrut[a], Xueqian Kong[c], Son-Jong Hwang[d], Matthew Neurock[b,2], and Alexander Katz[a,2]

[a]Department of Chemical and Biomolecular Engineering, University of California, Berkeley, CA 94720; [b]Departments of Chemical Engineering and Chemistry, University of Virginia, Charlottesville, VA 22904; [c]Environmental Energy Technologies Division, Lawrence Berkeley National Laboratory, Berkeley, CA 94720; and [d]Division of Chemistry and Chemical Engineering, California Institute of Technology, Pasadena, CA 91125

Edited* by Mark E. Davis, California Institute of Technology, Pasadena, CA, and approved November 12, 2012 (received for review July 11, 2012)

An approach for the control and understanding of supported molecular catalysts is demonstrated with the design and synthesis of open and closed variants of a grafted Lewis acid active site, consisting of Al(III)-calix[4]arene complexes on the surface of silica. The calixarene acts as a molecular template that enforces open and closed resting-state coordination geometries surrounding the metal active sites, due to its lower-rim substituents as well as site isolation by virtue of its steric bulk. These sites are characterized and used to elucidate mechanistic details and connectivity requirements for reactions involving hydride and oxo transfer. The consequence of controlling open versus closed configurations of the grafted Lewis acid site is demonstrated by the complete lack of observed activity of the closed site for Meerwein-Ponndorf-Verley (MPV) reduction; whereas, the open variant of this catalyst has an MPV reduction activity that is virtually identical to previously reported soluble molecular Al(III)-calix[4]arene catalysts. In contrast, for olefin epoxidation using *tert*-butyl-hydroperoxide as oxidant, the open and closed catalysts exhibit similar activity. This observation suggests that for olefin epoxidation catalysis using Lewis acids as catalyst and organic hydroperoxide as oxidant, covalent binding of the hydroperoxide is not required, and instead dative coordination to the Lewis acid center is sufficient for catalytic oxo transfer. This latter result is supported by density functional theory calculations of the transition state for olefin epoxidation catalysis, using molecular analogs of the open and closed catalysts.

molecular catalysis | single-site catalysts | MPVO reaction | organic-inorganic interface | selective oxidation

Metalloenzymes ubiquitously enforce a coordinatively unsaturated and open active site within the catalyst resting state (1); well-characterized examples of this include laccase (1), methane monooxygenase (2, 3), urease (4), and aconitase (5), among others. Open sites have historically been recognized as the relevant active sites in synthetic heterogeneous catalysts as well, typically consisting of metal surfaces (6), bulk inorganic oxides (7, 8), and heteroatom-substituted zeolites (9); however, control of heterogeneous catalyst function via selective synthesis of open sites has remained elusive, due in part to the challenge of synthesizing materials with programmable and well-defined structural environments at the active site on the atomic level. The importance of open active sites in heterogeneous catalysis is evident in the early work of Somorjai and coworkers, who comparatively characterized CO adsorption modes on open sites such as defect kinks and edge sites, as well as closed sites consisting of terraces, on crystalline Pt(111) surfaces (6). The former perform dissociative adsorption of CO, whereas associative adsorption of CO dominates on the latter (6), and this in turn has significant repercussions for understanding catalysis on Pt surfaces (10). Open sites have since been invoked as the relevant active sites in a variety of reactions including ammonia synthesis, oxidation, coking, and water–gas shift (11–14). There are several representative contemporary examples of open and closed heterogeneous catalyst active site structures in solid inorganic-oxide catalysts (*SI Appendix*, Fig. 1S). Within the context of this paper, open refers to active sites that are able to covalently bind a reactant via release of a labile monodentate ligand on the Lewis acid metal center; whereas, closed sites are unable to do this. A notable example of the catalytic significance of open active sites is provided by Corma et al. using Sn(β)-zeolite (15–18). Steaming of the fully condensed and closed Sn(IV) Lewis acid sites within the zeolite (*SI Appendix*, Fig. 1S entry 2b) likely hydrolyzes Sn−O−Si bonds, and thereby synthesizes open catalytically active sites (*SI Appendix*, Fig. 1S entry 2a) (15–18). Such open Sn (IV) sites have recently been characterized via FTIR spectroscopy using acetonitrile as a probe molecule, as well as solid-state NMR spectroscopy (19), and are hypothesized to be responsible for the high activity observed in heterogeneous MPV reduction (15–18), glucose isomerization to fructose via hydride transfer, (20, 21), and fructose dehydration to afford 5-(hydroxymethyl) furfural (22).

Here, we demonstrate the design and synthesis of both open and closed variants of a grafted Lewis acid site, using an organic–inorganic approach, which is based on grafted Al(III)-calix[4]arene active sites on the surface of partially dehydroxylated porous silica. Other notable examples of grafted metal cations on the silica surface include noncalixarene grafted Al(III) sites on silica using an aluminum-methyl precursor complex (23–25), and an elegant solid-phase version of the Sharpless homogeneous epoxidation catalyst (see below). This latter example employs open grafted Ta (V) active sites, which were shown to be highly enantioselective for epoxidation of allylic alcohols (26). Our approach is described with the synthesis and catalytic characterization of open and closed grafted active-site structures (*SI Appendix*, Fig. 1S entries 3a and 3b, respectively), and is first demonstrated for the MPV reduction shown. This is a reaction in which open sites are commonly invoked as a requirement for catalysis, to synthesize bound alkoxide via chemisorption of secondary alcohol to the Lewis acid site in a six-membered transition state. These open and closed active sites are subsequently used to help understand site-connectivity requirements in a system where it is currently unknown whether

Author contributions: P.N., W.T., A.O., X.K., S.-J.H., M.N., and A.K. designed research; P.N., W.T., A.O., X.K., S.-J.H., and M.N. performed research; P.N., W.T., A.O., X.K., S.-J.H., M.N., and A.K. contributed new reagents/analytic tools; P.N., W.T., M.N., and A.K. analyzed data; and P.N., W.T., M.N., and A.K. wrote the paper.

The authors declare no conflict of interest.

*This Direct Submission article had a prearranged editor.

[1]Present address: Corporate Strategic Research, ExxonMobil Research and Engineering, Annandale, NJ 08801.

[2]To whom correspondence may be addressed. E-mail: askatz@berkeley.edu or mneurock@gmail.com.

This article contains supporting information online at www.pnas.org/lookup/suppl/doi:10.1073/pnas.1211158110/-/DCSupplemental.

either open or closed sites are required for catalysis: Lewis acid–catalyzed olefin epoxidation using organic hydroperoxide as oxidant. This reaction as well as related Ti(IV)-catalyzed epoxidations using either homogeneous sites consisting of Ti(IV)-isopropoxide and tartrate (i.e., Sharpless epoxidation system, ref. 33) or Ti(IV) sites in zeolite TS-1 may prefer either the open or closed active-site structures for high activity (see *SI Appendix*, Fig. 1S entries 1a and 1b for open and closed structures, respectively); alternatively, they may function equally well with either one (27).

Early density functional theory (DFT) calculations of the TS-1 active site by Vayssilov and van Santen predict that a closed site catalyzes olefin epoxidation when using hydrogen peroxide as oxidant, without the need for cleavage of H−O hydroperoxide and Ti−O−Si bonds (28). This mechanism, as well as related recently proposed mechanisms involving organic hydroperoxide (29), are directly at odds with one proposed mechanism based on experimental evidence (30–32) (and supported with DFT modeling) (31, 32), which involves H−O-bond cleavage during hydrogen peroxide chemisorption and the open site (*SI Appendix*, Fig. 1S entry 1a) as a relevant intermediate. This latter mechanism closely resembles that proposed for Sharpless' Ti(IV)-catalyzed allylic alcohol epoxidation system, which also invokes an open active site; however, in the latter system, ^{17}O NMR spectroscopic data are inconclusive regarding the nature of hydrogen peroxide binding to the catalyst active site (i.e., covalent versus noncovalent hydrogen peroxide binding to the metal center) (33).

An understanding of the coordination requirements for catalyst active sites is invaluable to the rational design and implementation of new catalysts. In this article, the intentional synthesis of open and closed Lewis acid sites anchored on a solid surface enables the investigation of the kinetic consequences of each type of active-site structure for a particular reaction system. Density functional theory analysis of the relevant transition states for olefin epoxidation supports the experimentally observed effect of the open/closed nature of the catalyst resting state on the working-state catalytic activity. These results have broad implications on the covalent versus dative nature of hydroperoxide binding to the Lewis acid metal center during olefin epoxidation catalysis. The presented approach of synthesizing analogous complexes with and without open coordination sites provides an opportunity to investigate the coordination requirements for catalysis at the active site, which is otherwise difficult to assess experimentally.

Results and Discussion

The importance of sterically bulky and rigid calixarene-based ligands has recently been demonstrated in the design, synthesis, and stabilization of the most accessible metal clusters reported to date, as well as synthesis of stable open metal-carbonyl clusters in solution that are synthesized via decarbonylation, which can also be recarbonylated (34, 35). A conceptually related approach has been used to site isolate grafted metal cations on silica surfaces within non-octahedral coordination geometries, using Lewis acidic metallocalixarene complexes as precursors for anchoring (36, 37). Using the proven ability of *tert*-butyl-calix[4]arene ligands to site-isolate and template specific environments surrounding grafted metal cation catalysts on inorganic-oxide surfaces (36, 37), we synthesize both open and closed variants of a grafted metal catalyst active site (as represented by *SI Appendix*, Fig. 1S entries 3a and 3b).

Fig. 1 summarizes the synthesis of open and closed Al(III)-calix[4]arene active sites grafted on silica. Calix[4]arene ligand is selectively either bis- (in the case of 7) or tris- (in the case of 1) alkylated at the lower rim in a single step using cation templating during synthesis (38, 39). The resulting ligand is reacted with Me_3Al to afford the corresponding dimethyl-Al complex 2 (precursor for open heterogeneous site) or monomethyl-Al complex 8 (precursor for closed heterogeneous site) via evolution of methane. The final

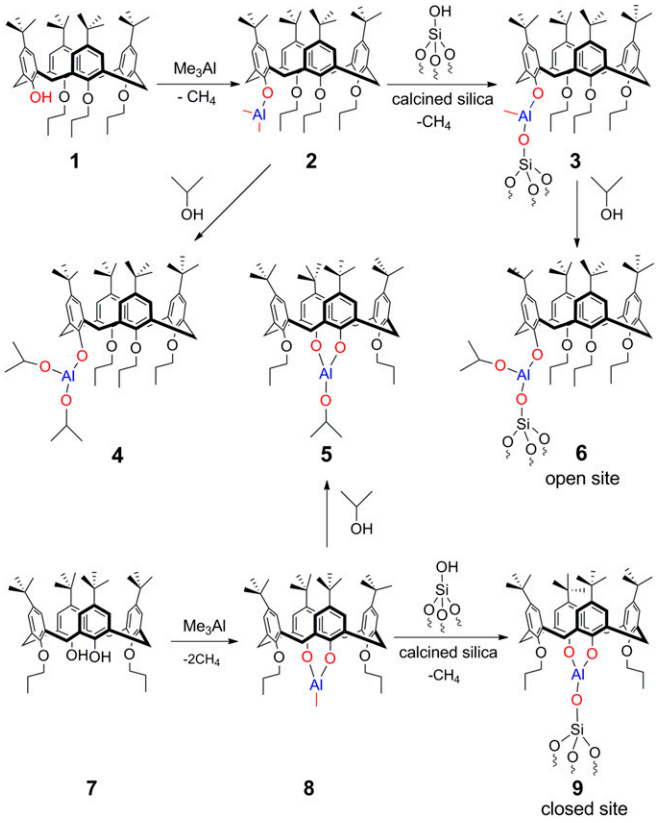

Fig. 1. Synthesis of open 6 and closed 9 Al(III) sites using calix[4]arene ligands. The homogeneous solution analogs 4 and 5 are synthesized by treating 2 and 8 with 2-propanol.

synthetic step involves grafting of methyl-Al species consisting of either 2 or 8 via reaction with silanol sites on dehydroxylated silica. This synthesizes grafted Al(III)-calix[4]arene sites within either an open 3 or a closed 9 configuration. Treatment of open grafted site 3 with isopropanol synthesizes open site 6 consisting of aluminum isopropoxide complex via liberation of methane. As an alternative, precursors 2 and 8 can be subsequently reacted with 2-propanol to yield soluble Al(III)-calix[4]arene isopropoxides 4 and 5, respectively.

Table 1 summarizes the open 6 and closed 9 heterogeneous catalysts investigated, consisting of varying surface coverage and dehydroxylated silica support pretreatments. Thermogravimetric analysis coupled with mass spectrometry (TGA) of materials 6 and 9 measures the amount of grafting on the surface of silica.

Table 1. Summary of materials synthesized

Sample*	μmol/g†	Calixarene nm^{-2}	Al‡:calixarene	MPV TOF§ h^{-1}
6-SiO_2-450	115	0.29		1.5
6-SiO_2-450	57	0.15	0.9	1.5
6-SiO_2-450	30	0.08		1.5
6-SiO_2-800	120	0.27		2.1
9-SiO_2-450	77	0.22	1.0	<0.03
9-SiO_2-450	117	0.33		<0.03

*Nomenclature: catalyst 9-SiO_2-450 indicates grafted complex 9 on silica pretreated to 450 °C before grafting.
†Active-site concentration: determined by combustion analysis using in-house TGA.
‡Measured by inductively coupled plasma mass spectrometry (ICP-MS).
§Turnover frequency (TOF) is number of MPV reduction events per time per Al site.

For both 6 and 9, the maximum surface coverage of grafted calix[4]arene complex on silica is ~0.3 calix[4]arene/nm^2, and elemental analysis confirms the expected Al:calixarene ratio of unity. Previously, we demonstrated a similar surface coverage of grafted metallocalixarene sites to correspond to the expected jamming limit for random sequential adsorption, at about 55% fractional surface area occupied by grafted calixarene sites. The thermal stabilities of 6 and 9 during combustion in air are similar as assessed using thermogravimetric analysis.

^{27}Al MAS NMR spectroscopy of the closed grafted Al(III)-calix[4]arene active site 9-SiO_2(450) is shown in Fig. 2*A*, and consists of a prominent resonance centered at ~33 ppm. The chemical shift of this resonance corresponds to previously reported five-coordinate aluminum centers in oxide materials (40, 41). Similar resonances are measured with spin-echo pulse sequence for methyl Al(III)-calixarene complexes before anchoring, as shown in Fig. 2*B* for closed material precursor 8 and Fig. 2*C* for open material precursor (see *SI Appendix* for corresponding spectra obtained with a single-pulse excitation). The broad ^{27}Al NMR patterns are a result of large ^{27}Al quadrupolar coupling in a low-symmetry coordination environment. The center resonances of all spectra in Fig. 2 are notably shifted away from 0 ppm, the expected chemical shift for octahedral aluminum species, and are within the range known for Al(III)-alkoxides and Al(III)-phenoxides (40, 41). There are no $AlMe_3$ species remaining after reaction as verified via complete loss of calix[4]arene OH resonance in the ^{1}H NMR spectra as well as lack of the characteristic 155-ppm resonance in the ^{27}Al NMR spectrum.

Homogeneous Al(III)-calix[4]arene complexes are active MPV reduction catalysts (42). Heterogeneous open catalyst 6 follows similar connectivity as previously described for related open homogeneous catalysts, among them 5, which also possesses a cone conformation, propoxy lower-rim substituents, and a covalent Al(III) attachment to the calix[4]arene lower rim via oxygen. The kinetic data for the MPV reduction of various heterogeneous and homogeneous catalysts are summarized in Fig. 3 and Table 1, using 2-chloroacetophenone and isopropanol as representative ketone and reductant, respectively, at room temperature. We observe closed variant heterogeneous 9-SiO_2(450) to be completely inactive for MPV reduction catalysis, as is aluminum isopropoxide grafted to silica. This confirms the closed nature of the

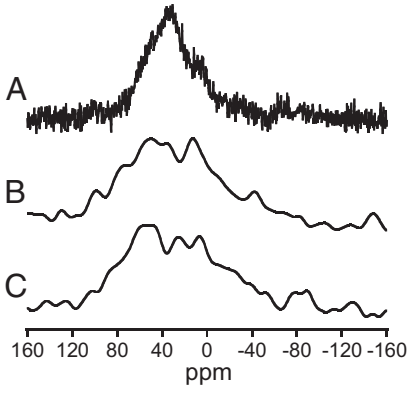

Fig. 2. (*A*) Solid-state ^{27}Al MAS NMR spectroscopy of 9-SiO_2(450) at room temperature; (*B*) liquid-state ^{27}Al NMR spectroscopy of 8 in d_8-toluene; (*C*) liquid-state ^{27}Al NMR spectroscopy of 2 in d_8-toluene. Liquid-state ^{27}Al NMR spectroscopy was performed on a 7.05 Tesla magnet, operating at a frequency of 78.2 MHz, and using 90° pulses of 2.2 μs. The spectra are obtained with a spin-echo sequence with an echo time of 40 μs (see *SI Appendix* for spectra obtained with single-pulse excitation of same precursors). The ^{27}Al chemical shift is calibrated to 1.1 M $Al(NO_3)_3$ in D_2O at 0 ppm, and Gaussian line broadening of 700 Hz is performed.

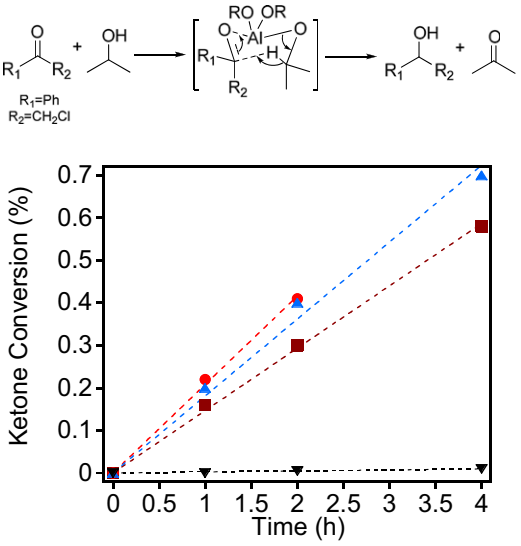

Fig. 3. MPV catalysis: open site 6-SiO_2-450 in brown (■), open site 6-SiO_2-800 in red (●), and closed 9-SiO_2-450 shown in black (▼), homogeneous catalysis with 5 in blue (▲). Grafted aluminum isopropoxide on silica has a negligible catalytic activity, which is similar to that observed for 9-SiO_2-450 for MPV reduction.

active site, which in 9-SiO_2(450) is enforced via design of the calixarene ligand as molecular template.

In stark contrast, catalysis using open catalyst 6 follows the previously observed and expected pseudozero-order rate dependence on ketone concentration (42). The turnover frequency for catalyst 6-SiO_2(800) is virtually the same as that observed for homogeneous catalyst 5. No detectable leaching of the catalyst is observed via hot-filtration test during catalysis (performed at reaction temperature—see *SI Appendix* for details). When comparing 6-SiO_2(450) as catalyst at either dilute or saturation surface coverage of grafted Al(III)-calix[4]arene sites, there is no coverage dependence on the turnover frequency (*SI Appendix*). These data are consistent with the single-site nature of 6-SiO_2(450) as catalyst, as observed for other grafted metallocalixarene-on-silica catalysts (36). In addition, the slightly lower rate for 6-SiO_2(450) relative to 6-SiO_2(800) suggests that a high degree of silica dehydroxylation may promote monodentate attachment of open precursors to the silica surface, because bidentate grafting is expected to synthesize MPV-inactive sites within a closed configuration. A monodentate mode of attachment of the open Al(III) sites to silica within catalyst 6 is consistent with studies of previous investigators who have grafted Me_3Al on silica (23–25), and a recent detailed ^{27}Al NMR spectroscopic analysis of the binding of Et_3Al on silica, which shows the predominant grafted species to contain two ethyl ligands on aluminum (40). Scott et al. have notably shown within this regard that a silica dehydroxylation temperature of 800 °C promotes greater monodentate grafting of organometallic complexes relative to a lower temperature of 500 °C (23, 24). The observations above rationalize the need for steaming, to open the coordination sphere surrounding heterogeneous Lewis acid active sites, when using Sn-β zeolite as catalyst for MPV reduction (15–18).

For the heterogeneous catalyst consisting of aluminum isopropoxide grafted onto silica, the active sites are closed presumably due to extensive aggregation. Such aggregation has been previously reported to occur in dilute air-free solution of aluminum isopropoxide (43), and can be envisioned to only be amplified at the high local concentrations of grafted species on the silica surface. This comparison highlights the critical role of the calixarene as a ligand that enforces isolation of the catalyst active sites within a preferred coordination geometry, in a manner

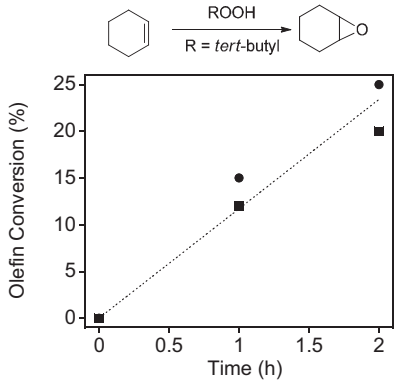

Fig. 4. Activity of epoxidation of cyclohexene using *tert*-butylhydroperoxide as oxidant in toluene at 60 °C, using closed 9-SiO_2-800 (●) and open 10-SiO_2-800 (■) as grafted calix[4]arene catalyst active site. The linear trend fitting all data using least-squares regression is represented by the dashed line for ease of comparison.

that cannot be accomplished via conventional methods of grafting cations.

The results above demonstrate the synthesis and function of a closed grafted active site, which is unable to perform MPV catalysis because of its inability to chemisorb isopropanol as isopropoxide, as well as an open grafted active site that is catalytically active for MPV reduction. For olefin epoxidation catalysis using organic hydroperoxide as oxidant, it is unclear whether either open or closed connectivity at the active site in the working state is required for catalysis. These issues are relevant to heterogeneous epoxidation catalysis using zeolite catalyst TS-1 as well as homogeneous catalysis with Sharpless' system (33). In all of these systems, it remains unclear whether an open versus closed active site is required for epoxidation catalysis (i.e., whether productive hydroperoxide binding for epoxidation catalysis involves covalent Ti−O−OR binding versus dative Ti···HOOR oxidant coordination to the Lewis acid metal center). Dative hydroperoxide coordination could certainly proceed with a closed active site such as 9. However, covalent peroxide coordination is expected to require an open active site such as 6, in the absence of Al−O−Si or Al−O−calix[4]arene bond-breaking reactions with organic hydroperoxide. Such bond breaking is not observed even in the presence of large excesses of isopropanol in the MPV reduction systems described above, because the closed active site would otherwise have been an active catalyst for MPV reduction.

Fig. 4 shows the results of cyclohexene epoxidation using *tert*-butyl-hydroperoxide as oxidant, on both open and closed grafted Al(III)-calix[4]arene active sites as catalysts. In contrast to the connectivity requirements for MPV reduction catalysis, both open and closed heterogeneous active sites are similarly active for olefin epoxidation catalysis, which is shown by the slope of the dashed line in Fig. 4. The epoxidation rate constant corresponding to the open 10-SiO_2-800 and closed 9-SiO_2-800 catalysts in Fig. 4 is 0.275 M^{-2} s^{-1}. This rate constant is about 30-fold lower compared with previously reported grafted Ti(IV)-calix[4]arene on silica epoxidation catalysts.

A possible interpretation of the olefin epoxidation result in the previous paragraph is that rates for open and closed catalysts are nearly equal because of interconversion of the closed resting state of the active site of 9 to an open working configuration during olefin epoxidation catalysis, presumably via either Si−O−Al or Al−O−calix[4]arene bond breaking by the hydroperoxide to synthesize a covalently bound Al(III)-alkylperoxide intermediate. We use the following control experiment to investigate whether such a scenario is likely to occur during catalysis. First, epoxidation of cyclohexene using *tert*-butyl-hydroperoxide as oxidant and closed site 9-SiO_2-800 as catalyst is conducted. The used catalyst after this epoxidation is subsequently used a second time for MPV reduction. If epoxidation conditions open up the closed site 9, there should be observable MPV reduction catalysis activity following use of the catalyst for olefin epoxidation; however, no such activity is observed experimentally. Given the large amount of catalyst used in this control experiment (12 mol percent relative to ketone substrate), MPV reduction activity would be detected even for a single active-site turnover event in this instance. This result is consistent with the closed site 9 remaining intact as a closed site within the working state during olefin epoxidation reaction conditions. Therefore, the similar observed activity of open and closed for olefin epoxidation using *tert*-butylhydroperoxide as oxidant in Fig. 4 is unlikely to be due to an interconversion of closed catalyst into an open state during epoxidation catalysis.

The equivalence of the catalytic activity of open and closed sites above suggests that covalent peroxide binding to the metal center may not be a necessity for olefin epoxidation reactions when using organic hydroperoxide as oxidant, and instead points to nondissociative adsorption of the hydroperoxide to the Lewis acid center during epoxidation catalysis. Nonlocal gradient corrected DFT calculations of olefin epoxidation were conducted to determine the activation barriers and the reaction energies for both closed catalyst 9 and open catalyst bound with organic peroxide 10, as shown in Fig. 5, to confirm such a hypothesis. The computational details are described in *SI Appendix*. The catalyst models use either the $-O-SiH_3$ or the $-O-Si(SiH_3)_3$ cluster as a reliable surrogate for silica in active site as the reactions demonstrate very little charge separation or longer range electronic interactions (44). Calculations with the larger $-Si(OSiH_3)_3$ cluster models of the silica, i.e., 11 for open and 12 for closed as shown in Fig. 5 result in changes in activation and reaction energies that are less than 1 kcal/mol. Both cases consisting of one equivalent of organic hydroperoxide and two equivalents (e.g., one equivalent in excess) of organic hydroperoxide relative to Al(III)-calix[4]arene active sites are considered, and ethylene is the olefin reactant.

The activation energy calculated for open site 11 is 10.6 kcal/mol, whereas for closed site 12, it is 10.0 kcal/mol. The comparable activation energies when using either open or closed catalyst active sites reinforce the direct mechanism of Lewis acid–catalyzed epoxidation, which is supported by the results of experiments using heterogeneous catalysts 6 and 9 above. Such a result is also consistent with the mechanism of ethylene epoxidation catalysis that is observed when using *tert*-butylhydroperoxide as oxidant and $Ti(OSi(CH_3)_3)_4$ as soluble catalyst by Urakawa and coworkers (29), as well as the original DFT studies by Vayssilov and van Santen on TS-1–catalyzed epoxidation of ethylene, which found that the barrier for oxo transfer via deprotonation of hydroperoxide

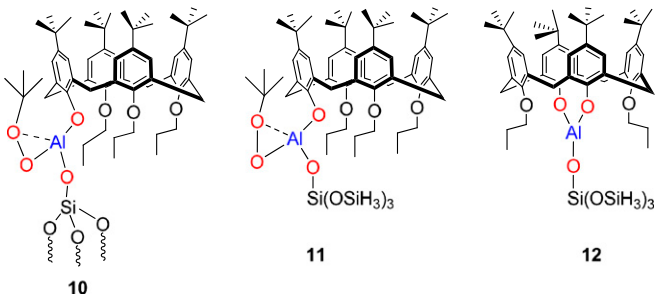

10 11 12

Fig. 5. Representation of molecular structures used for nonlocal gradient corrected DFT calculations of olefin epoxidation. The grafted active site 10 is modeled with molecule 11, consisting of open site with bound organic peroxide, and the corresponding closed catalyst active site molecular model is represented by 12.

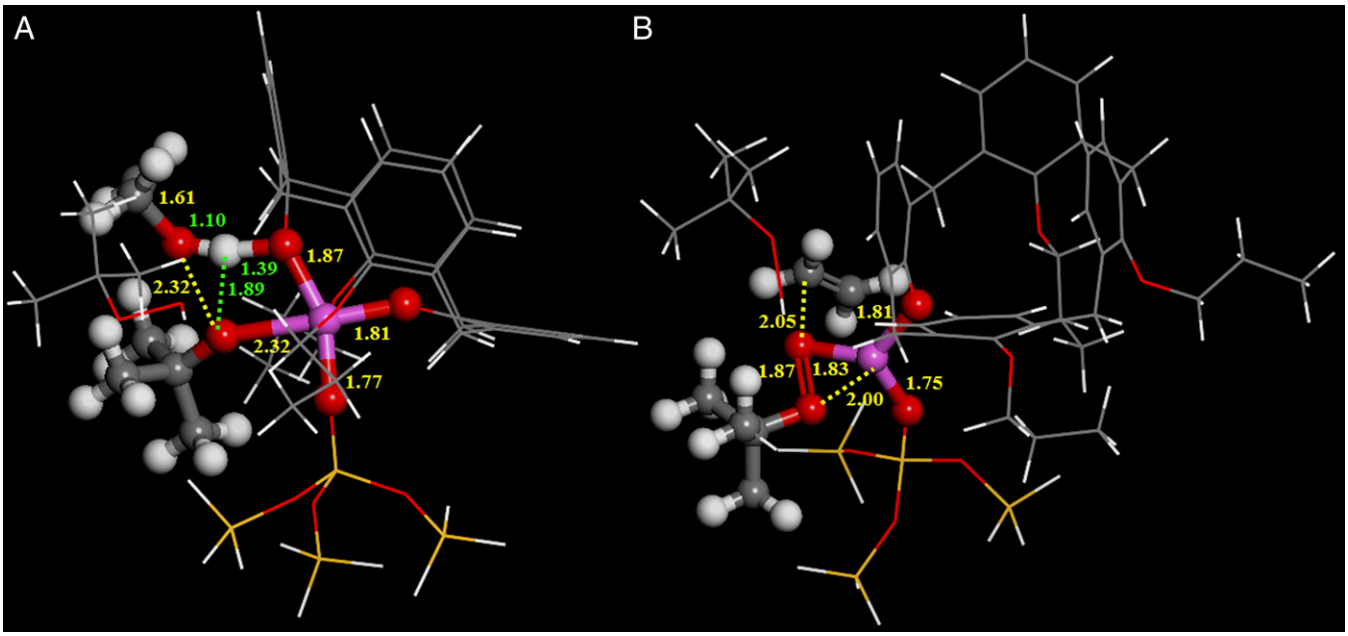

Fig. 6. DFT-calculated transition-state structures for the (*A*) closed using 12 and (*B*) open using 11 forms of the active sites grafted on silica for the Al(III)-catalyzed epoxidation of ethylene with *tert*-butylhydroperoxide. The structures refer to case with an extra equivalent of the hydroperoxide present. Purple, red, gray, white, and yellow spheres (or lines) refer to Al, O, C, H, and Si atoms, respectively. The transition state in (*A*) for closed occurs much later than in (*B*) for open. DFT-calculated activation barriers are 10.0 and 10.6 kcal/mol for the transition states shown in (*A*) for closed and (*B*) for open. The extra equivalent of organic hydroperoxide acts to decrease energy barriers by about 4 kJ/mol as a result of weak hydrogen bonding that stabilizes the transition states. The weak hydrogen-bonding stabilization is consistent with results reported by Urakawa and coworkers (29) and Lundin and coworkers (47, 48).

is higher by 1.7 kcal/mol compared with the mechanism with non-dissociatively bound hydroperoxide (28).

The relevant details of the transition-state structures for the case consisting of an extra equivalent of *tert*-butylhydroperoxide are shown in Fig. 6 (*SI Appendix*, Fig. 2S for summary of calculation results and calculation data on cases with and without an extra equivalent of organic hydroperoxide). For both the open and closed structures, the extra equivalent of hydroperoxide lowers the transition-state energy via hydrogen-bond–donating interactions to the hydroperoxide involved in oxygen transfer, as described previously (29), and this additional transition-state energy lowering corresponds to ~0.6–1.0 kcal/mol. We note that the hydrogen bond donor within this context can in principle be either organic hydroperoxide, alcohol byproduct of organic hydroperoxide that is formed following oxygen transfer, or silanol (30–33). Previous comparisons of trimethylsilyl (TMS)-capped and native silanol-containing Ti-on-silica olefin epoxidation catalysts show a lack of appreciable activity or selectivity difference under dry conditions, when using organic hydroperoxide as oxidant (45). Because such TMS capping is known to block virtually all accessibility of silanols to serve as hydrogen bond donors (46), this result suggests that either organic hydroperoxide or alcohol byproduct can serve at least as an effective hydrogen bond donor as a surface silanol for decreasing the barrier for oxygen transfer.

The transition-state structures for open 11 and closed 12 show similar bond distances between bridging oxygen ligands and the Al metal center, involving the oxygen atoms of the calix[4]arene (1.81 Å open vs. 1.87 and 1.81 Å closed) and Si atom (1.75 Å for open and 1.77 Å for closed), and these distances are consistent with expected covalent distances. This suggests a lack of either Al−O−Si or Al−O−calix[4]arene bond breaking at the transition state for the closed active site 12. This is further reinforced by the dative bond distance of 2.32 Å between Al(III) and the oxygen connected to the *tert*-butyl fragment for the closed transition state, which is significantly larger than the analogous distance of 2.00 Å for the open transition state. This strong dative bond in the closed 12 transition state presumably provides the crucial negative charge delocalization on the forming OR^- fragment during oxygen transfer (47, 48). There is a significant lengthening of one of the dative Al···OPr bonds on the calix[4]arene lower rim relative to the other in the closed transition state (2.22 versus 2.37 Å), which allows the hydroperoxide to approach closer into the Al(III) center and establish the aforementioned dative contact with the Lewis acid in the transition state. The transition state for the closed structure appears to occur much later along the reaction path than that for the open site, as the C−O bonds of the ensuing epoxide are 1.61 and 2.05 Å, for closed and open transition states, respectively. The relatively longer C−O bond in the open form is the result of the stronger stabilization of the O that forms the epoxide by the Al center. The oxygen on the epoxide in the transition state of the closed form is stabilized instead by the proton that results from the hydroperoxide and has little interaction with the Al center.

In summary, we demonstrate the synthesis by design of open and closed variants of a grafted Lewis acid site on the surface of silica, where the isolation and structure of the active site are enforced using a bulky calix[4]arene as molecular template. We demonstrate control of MPV reduction catalysis using these active sites and subsequently use this approach as a tool to investigate active site requirements for olefin epoxidation catalysis. Both experimental results as well as DFT calculations are consistent with similar barriers for open and closed sites, and support a non-dissociative hydroperoxide binding for Lewis acid–catalyzed olefin epoxidation on closed active sites.

Materials and Methods

A description of (*i*) synthesis of open catalyst 6-SiO_2 and closed catalyst 6-SiO_2 active sites, and (*ii*) procedure used for olefin epoxidation and MPV reduction catalysis is included in *SI Appendix*. These syntheses and procedures are based on established literature precedent. See refs. 36, 37, and 42.

ACKNOWLEDGMENTS. A.K. acknowledges helpful conversations with Dr. Karl Mueller and Dr. Nancy Walton (Pacific Northwest National Laboratory) regarding interpretation of ^{27}Al MAS NMR spectra. W.T. acknowledges the

Texas Advanced Computing Center for Extreme Science and Engineering Discovery Environment (XSEDE) computing resources. The authors thank Prof. Jeffrey A. Reimer (University of California, Berkeley) for his expertise with liquid-phase ^{27}Al NMR experiments and the Office of Basic Energy Sciences of the US Department of Energy (Grant DE-FG02-05ER15696) for support of this work. The Caltech Solid-State NMR Facility is supported by the National Science Foundation (NSF) under Grant 9724240 and is partially supported by the Materials Research Science and Engineering program of NSF (Grant DMR-520565).

1. Quintanar L, et al. (2005) Spectroscopic and electronic structure studies of the trinuclear Cu cluster active site of the multicopper oxidase laccase: Nature of its coordination unsaturation. *J Am Chem Soc* 127(40):13832–13845.
2. Yoshizawa K, Ohta T, Yamabe T, Hoffman R (1997) Dioxygen cleavage and methane activation on diiron enzyme models: A theoretical study. *J Am Chem Soc* 119: 12311–12321.
3. Lee D, Lippard SJ (1998) Structural and functional models of the dioxygen-activating centers of non-heme diiron enzymes ribonucleotide reductase and soluble methane monooxygenase. *J Am Chem Soc* 120:12153–12154.
4. Karplus PA, Pearson MA, Hausinger RP (1997) 70 years of crystalline urease: What have we learned? *Acc Chem Res* 30:330–337.
5. Beinert H (2000) Iron-sulfur proteins: Ancient structures, still full of surprises. *J Biol Inorg Chem* 5(1):2–15.
6. Iwasawa Y, Mason R, Textor M, Somorjai GA (1976) The reactions of carbon monoxide at coordinatively unsaturated sites on a platinum surface. *Chem Phys Lett* 44:468–470.
7. Burwell RL, Haller GL, Taylor KC, Read JF (1969) Chemisorptive and catalytic behavior of chromia. *Adv Catal* 20:1–96.
8. Over H, et al. (2000) Atomic-scale structure and catalytic reactivity of the RuO_2(110). *Science* 287:1474–1476.
9. Zecchina A, Rivallan M, Berlier G, Lamberti C, Ricchiardi G (2007) Structure and nuclearity of active sites in Fe-zeolites: Comparison with iron sites in enzymes and homogeneous catalysts. *Phys Chem Chem Phys* 9(27):3483–3499.
10. Bratlie KM, Lee H, Komvopoulos K, Yang P, Somorjai GA (2007) Platinum nanoparticle shape effects on benzene hydrogenation selectivity. *Nano Lett* 7(10):3097–3101.
11. Jacobsen CJH, et al. (2000) Structure sensitivity of supported ruthenium catalysts for ammonia synthesis. *J Mol Catal A* 163:19–26.
12. Deng X, Min BK, Guloy A, Friend CM (2005) Enhancement of O_2 dissociation on Au111 by adsorbed oxygen: Implications for oxidation catalysis. *J Am Chem Soc* 127(25):9267–9270.
13. Lu J, et al. (2012) Coking- and sintering-resistant palladium catalysts achieved through atomic layer deposition. *Science* 335(6073):1205–1208.
14. Shekhar M, et al. (2012) Size and support effects for the water-gas shift catalysis over gold nanoparticles supported on model Al_2O_3 and TiO_2. *J Am Chem Soc* 134(10): 4700–4708.
15. Corma A, Domine ME, Valencia S (2003) Water-resistant solid Lewis acid catalysts: Meerwein-Ponndorf-Verley and Oppenauer reactions catalyzed by tin-beta zeolite. *J Catal* 215:294–304.
16. Boronat M, Concepcion P, Corma A, Renz M, Valencia S (2005) Determination of the catalytically active oxidation Lewis acid sites in Sn-beta zeolites, and their optimization by the combination of theoretical and experimental studies. *J Catal* 234:111–118.
17. Corma A, Domine ME, Nemeth L, Valencia S (2002) Al-free Sn-beta zeolite as a catalyst for the selective reduction of carbonyl compounds (Meerwein-Ponndorf-Verley reaction). *J Am Chem Soc* 124(13):3194–3195.
18. Corma A, Renz M (2005) Experimental evidence for a dual site mechanism in Sn-beta and Sn-MCM-41 catalysts for the Baeyer-Villiger oxidation collect. *Collect Czech Chem Commun* 70:1728–1736.
19. Bermejo-Deval R, et al. (2012) Metalloenzyme-like catalyzed isomerizations of sugars by Lewis acid zeolites. *Proc Natl Acad Sci USA* 109(25):9727–9732.
20. Moliner M, Román-Leshkov Y, Davis ME (2010) Tin-containing zeolites are highly active catalysts for the isomerization of glucose in water. *Proc Natl Acad Sci USA* 107(14):6164–6168.
21. Román-Leshkov Y, Moliner M, Labinger JA, Davis ME (2010) Mechanism of glucose isomerization using a solid Lewis acid catalyst in water. *Angew Chem Int Ed Engl* 49(47):8954–8957.
22. Nikolla E, Román-Leshkov Y, Moliner M, Davis ME (2011) "One-pot" synthesis of 5-(hydroxymethyl)furfural from carbohydrates using tin-beta zeolite. *ACS Catal* 1:408–410.
23. Scott SL, Church TL, Nguyen DH, Mader EA, Moran J (2005) An investigation of catalyst/cocatalyst/support interactions in silica supported olefin polymerization catalyst based on Cp*$TiMe_3$. *Top Catal* 34:109–120.
24. Fleischman SD, Scott SL (2011) Evidence for the pairwise disposition of grafting sites on highly dehydroxylated silicas via their reactions with $Ga(CH_3)_3$. *J Am Chem Soc* 133(13):4847–4855.
25. Anwander R, Palm C, Groeger O, Engelhardt G (1998) Formation of Lewis acidic support materials via chemisorption of trimethylaluminum on mesoporous silicate MCM-41. *Organometallics* 17:2027–2036.
26. Meunier D, Piechaczyk A, Basset JM, de Mallmann A (1999) Silica-supported tantalum catalysts for asymmetric epoxidations of allyl alcohols. *Angew Chem, Int Ed Engl* 38(23):3540–3542.
27. Bordiga S, Bonino F, Damin A, Lamberti C (2007) Reactivity of Ti(IV) species hosted in TS-1 towards H_2O_2-H_2O solutions investigated by ab initio cluster and periodic approaches combined with experimental XANES and EXAFS data: A review and new highlights. *Phys Chem Chem Phys* 9(35):4854–4878.
28. Vayssilov GN, van Santen RA (1998) Catalytic activity of titanium silicalites—A DFT study. *J Catal* 175:170–174.
29. Urakawa A, Bürgi T, Skrabal P, Bangerter F, Baiker A (2005) Interaction of water, alkyl hydroperoxide, and allylic alcohol with a single-site homogeneous Ti-Si epoxidation catalyst: A spectroscopic and computational study. *J Phys Chem B* 109(6): 2212–2221.
30. Clerici MG, Ingallina P (1993) Epoxidation of lower olefins with hydrogen peroxide and titanium silicalite. *J Catal* 140:71–83.
31. Wells DH, Jr., Joshi AM, Delgass WN, Thomson KT (2006) A quantum chemical study of comparison of various propylene epoxidation mechanisms using H_2O_2 and TS-1 catalyst. *J Phys Chem B* 110(30):14627–14639.
32. Neurock M, Manzer LE (1996) Theoretical insights on the mechanism of alkene epoxidation by H_2O_2 with titanium silicalite. *Chem Commun (Cambridge, UK)* (10): 1133–1134.
33. Finn MG, Sharpless KB (1991) Mechanism of asymmetric epoxidation. 2. Catalyst structure. *J Am Chem Soc* 113:113–126.
34. de Silva N, et al. (2010) A bioinspired approach for controlling accessibility in calix[4]arene-bound metal cluster catalysts. *Nat Chem* 2(12):1062–1068.
35. Okrut A, et al. (2012) Stabilization of coordinatively unsaturated Ir_4 clusters with bulky calix[4]arene phosphine ligands: A comparative study of mechanical and chemical effects. *Dalton Trans* 41:2091–2099.
36. Notestein JM, Iglesia E, Katz A (2004) Grafted metallocalixarenes as single-site surface organometallic catalysts. *J Am Chem Soc* 126(50):16478–16486.
37. de Silva N, Hwang SJ, Durkin KA, Katz A (2009) Vanadocalixarenes on silica: Requirements for permanent anchoring and electronic communication. *Chem Mater* 21: 1852–1860.
38. Iwamoto K, Shinkai S (1992) Syntheses and ion selectivity of all conformational isomers of Tetrakis((ethoxycarbonyl)methoxy)calix[4]arene. *J Org Chem* 57:7066–7073.
39. Iwamoto K, Yanagi A, Araki K, Shinkai S (1991) Syntheses of new isomers from *para t*-Butylcalix[4]arene. Strategies for regioselective alkylation on the lower rim. *Chem Lett* 20:473–476.
40. Kerber RN, et al. (2012) Nature and structure of aluminum surface sites grafted on silica from a combination of high-field aluminum-27 solid-state NMR spectroscopy and first-principles calculations. *J Am Chem Soc* 134(15):6767–6775.
41. Kriz O, Casensky B, Lycka A, Fusek J, Hermanek S (1984) ^{27}Al NMR behavior of aluminum oxides. *J Magn Reson* 65:371–381.
42. Nandi P, et al. (2011) Molecular effect of ketone binding on MPV reduction using Al(III)-Calix[4]arene Lewis acids. *J Catal* 284:42–49.
43. Shiner VJ, Whittaker D (1963) The mechanism of the Meerwein-Ponndorf-Verley reaction. *J Am Chem Soc* 85:2337.
44. Cheal K, Traylor TG, Perrin CL (1998) mCPBA epoxidation of alkenes: Reinvestigation of correlation between rate and ionization potential. *J Am Chem Soc* 120:9513–9516.
45. Corma A, et al. (1998) Strategies to improve the epoxidation activity and selectivity of Ti-MCM-41. *Chem Commun (Cambridge, UK)* (20):2211–2212.
46. Bass JD, Anderson SL, Katz A (2003) The effect of outer-sphere acidity on chemical reactivity in a synthetic heterogeneous base catalyst. *Angew Chem, Int Ed Engl* 42(42): 5219–5222.
47. Lundin A, Panas I, Ahlberg E (2009) Quantum chemical modeling of propene and butene epoxidation with hydrogen peroxide. *J Phys Chem A* 113(1):282–290.
48. Lundin A, Panas I, Ahlberg E (2007) Quantum chemical modelling of ethene epoxidation with hydrogen peroxide: role of catalytic sites. *Phys Chem Chem Phys* 9(45): 5997–6003.